HHS Public Access

Author manuscript

J Immunol. Author manuscript; available in PMC 2021 March 01.

Published in final edited form as:

J Immunol. 2020 March 01; 204(5): 1085–1090. doi:10.4049/jimmunol.1901260.

The RNA-Binding Protein EWS is a Novel Modulator of Lymphotoxin-β Receptor Signaling

Richard Virgen-Slane[*], **Ricardo G. Correa**[*], **Parham Ramezani-Rad**[‡], **Seth Steen-Fuentes**[*], **Thiago Detanico**[*], **Michael J. DiCandido**[§], **Jun Li**[§], **Carl F. Ware**[*,¶]

[*] Laboratory of Molecular Immunology, Infectious and Inflammatory Diseases Center and Sanford Burnham Prebys Medical Discovery Institute, 10901 North Torrey Pines Rd., La Jolla, CA 92037, USA

[‡] NCI-Designated Cancer Center, Sanford Burnham Prebys Medical Discovery Institute, 10901 North Torrey Pines Rd., La Jolla, CA 92037, USA

[§] Department of Immunology & Respiratory Disease Research, Boehringer Ingelheim Pharmaceuticals, Inc. 900 Ridgebury Road, Ridgefield, CT 06877, USA.

Abstract

Lymphotoxin β receptor (LTβR) signaling is crucial for lymphoid tissue organogenesis and immune homeostasis. To identify novel regulatory mechanisms for signaling, we implemented a two-step screen that uses co-expression analysis of human fibroblasts undergoing LTβR stimulation and affinity-purification mass spectrometry (AP-MS) for the LTβR signaling protein, TNF receptor-associated factor 3 (TRAF3). We identify Ewing's sarcoma (EWS) protein as a novel LTβR signaling component that associates with TRAF3, but not with TNF receptor-associated factor 2 (TRAF2). The EWS:TRAF3 complex forms under unligated conditions that is disrupted following activation of the LTβR. We conclude that EWS limits expression of pro-inflammatory molecules, GM-CSF and ERK-2, promoting immune homeostasis.

- EWS functions as a modulator downstream of LTβR stimulation.
- TRAF3, but not TRAF2, links EWS to receptor activation.
- EWS controls inflammatory responses mediated by GM-CSF

Introduction

LTβR is a member of the TNF Receptor Superfamily (TNFRSF), which coordinates gene activation for lymphoid tissue differentiation, homeostasis, and immune responses [Reviewed in (1)]. Ligation of the LTβR by the cytokines TNF ligand superfamily member

[¶] To whom correspondence should be addressed: Carl F. Ware, Infectious and Inflammatory Diseases Center, Sanford Burnham Prebys Medical Discovery Institute, 10901 North Torrey Pines Rd., La Jolla, CA 92037, USA. Tel: (858) 795-5335; cware@sbpdiscovery.org.

Disclosures

The authors disclose support for this project was provided in part by Boehringer Ingelheim with a research contract to Sanford Burnham Prebys Medical Discovery Institute. C.F.W. served as Principal Investigator of the contract and has no other potential conflict of interest with Boehringer Ingelheim; M.J.D. and J.L. are employees of Boehringer Ingelheim. The funder had the following involvement with the study: experimental design, data acquisition, and analysis.

14 (LIGHT) or Lymphotoxin-$\alpha_1\beta_2$ induces receptor clustering, which activates NF-κB transcription factors [Reviewed in (2)]. For the classical NF-κB pathway, inhibitor of NF-κB kinase subunits alpha and beta phosphorylate IκB, inducing its degradation, which allows the nuclear translocation of NF-κB subunits. Pro-longed LTβR stimulation also induces allosteric regulation of the TRAF3:TRAF2 complex, leading to its autoubiquitination and degradation (3). In this scenario, NF-κB-inducing kinase (NIK) is no longer targeted for proteasome-dependent degradation by TRAF3:TRAF2, leading to phosphorylation of NF-κB-2 (p100), which is processed into p52 in a proteasome-dependent manner. Collectively, this pathway is known as the alternative (non-canonical) NF-κB pathway [Reviewed in (2)].

Accumulating evidence shows that LTβR also contributes to autoimmune pathology (4), including the formation of ectopic clusters of organized lymphoid tissue that form at sites of chronic inflammation. Additionally, stimulation of LTβR in rheumatoid arthritis fibroblast-like synoviocytes amplifies inflammation through the production of ICAM, IL-8, and CCL-2 (5, 6). Induction of a steroid-resistant inflammatory phenotype in human lung epithelial cells is driven by stimulation of LTβR (7). Furthermore, blockade of LTβR signaling resolves the type I IFN signature in rheumatoid arthritis patients (8). Understanding the determinants for LTβR signaling, which distinguish its homeostatic functions from its roles in autoimmunity may elucidate novel strategies for controlling autoimmune disease.

In this work, we implemented a two-step method for identifying candidate regulators of the LTβR pathway. We first used transcriptomics with weighted correlation network analysis (WGCNA) to detect gene modules in Normal Human Dermal Fibroblasts (NHDF) undergoing LTβR stimulation. To identify a potential link between modules that may be regulated by the LTβR pathway at the protein level, we focused on signaling inhibitor, TRAF3. With this strategy, we identify EWS (encoded by *EWSR1*) as a novel component of the LTβR pathway. Depletion of EWS altered NF-κB responsiveness to LTβR stimulation, elevated expression of ERK-2 signaling protein, and caused aberrant induction of GM-CSF.

Materials and Methods

Antibodies and reagents

Stimulation: LIGHT (664-LI R&D systems), goat anti-human LTβR antibody (9). Detection antibodies: Cell Signaling Technology (EWS 11910, phospho-ERK-1/−2 9101, phospho-p38 9211), Santa Cruz Biotechnology (EWS sc-28327 AF647, TRAF3 sc-1828), Thermo (TRAF3 12H13L59), Abcam (p100 ab32859), and Sigma (Actin A2228).

AP-MS and Bayesian Network (BN) learning

Proteomics performed by Sanford Burnham Prebys Proteomics Core. Nonspecific proteins were removed using SaintExpress (10) and Crapome (11); discretized into three levels, and subjected to a tabu search with bootstraping via bnlearn (12). Inverse relationships were detected by BN inference using the gRain package in R (13).

Expression Plasmids

EWS-myc expressed, from pcDNA3.1 EWS-myc-HIS (14), which was a gift from Heinz Gehring (Addgene plasmid # 46386). For FLAG-tagged proteins, pcDNA3.1(+)-FLAG-TRAF3 and pcDNA3.1(+)-FLAG-TRAF2 were used (3). Human LTβR and HVEM expressed from pcDNA3.1 and pcDNA3 vectors, respectively.

Protein analysis

Tagged proteins were isolated from Human embryonic kidney 293T (HEK293T) using Sigma (A2220). Endogenous EWS was isolated from HeLa cells using Santa Cruz (sc-398318) with Dynabead Protein G (ThermoFisher Scientific).

Quantitative RT-PCR, secretion, and RNA interference

GM-CSF expression was measured with primers (7) in reference to *L32*, forward: GGATCTGGCCCTTGAACCTT, and reverse: GAAACTGGCGGAAACCCA primers. GM-CSF was measured using the Luminex platform. Standards were used with drlumi to estimate absolute protein levels (15). Plasmids expressing shEWS A, shEWS B, or shCtrl were purchased from G.E. Dharmacon (V3LHS_641851, V3LHS_641854, or RHS4346, respectively). For siRNA, pools targeting *EWS* or Null were purchased from G.E. Dharmacon (L-005119–02 and D-001810–10-05).

Statistics and WGCNA

Differential expression analysis of nCounter human inflammation panel (GSE110102 via https://www.ncbi.nlm.nih.gov/geo/) was carried out using DESeq2 with Wald and Benjamini-Hochberg p-value adjustment (cut off = 0.1) (16). All statistical analysis for quantitative RT-PCR and western blots was done in R using linear regression. RNAseq data were normalized using rlog variance stabilization (16) and analyzed using WGCNA package in R (17) with a soft-power threshold of seven (Supplemental Fig. 1A). Module names were then selected by the most significant GO enrichment term (ontology size cut off = 150) using the GOstats package in R (18).

Results and *Discussion*

‘Omics screen links EWSR1 to LTβR-TRAF3 pathway

WGCNA calculates gene-gene relationships from global expression data to segregate genes into functional groups called modules (17). Each module has a “hub”, which is a gene with high influence over other genes within its module (17). Because of the importance of a hub for module function, we started our screen by identifying hubs in cells undergoing LTβR signaling (Fig. 1A Top). We detected a total of 39 candidate gene hubs (Supplemental Fig. 1B), representing the 39 modules linked to LTβR signaling (Fig. 1A Bottom).

Next, we proceeded to identify candidates that were linked to TRAF3. We focused on TRAF3 for two reasons. First, it is a major inhibitor of LTβR signaling and its depletion is concomitant with activation (19). Second, the TRAF3:TRAF2 and TRAF3:NIK complexes formed in the absence of active LTβR signaling mediate this inhibitory role of TRAF3. Thus, we carried out an AP-MS study that focused on identifying TRAF3 complexes formed

in the absence of LTβR signaling. A TRAF3 variant with the F474E substitution (TRAF3-M; Supplemental Fig. 1C), which blocks binding to LTβR (3), was included to find interactions that may be influenced by receptor binding (Supplemental Fig. 1D). We filtered for binary interactions (Supplemental Table I), and predicted distinct complexes using BN learning with Bayesian inference (Fig. 1B). A total of nine candidates linked to TRAF3 were detected.

We cross-referenced the 39 module hubs detected by WGCNA with the nine TRAF3-binding proteins detected by our AP-MS study, identifying EWS as a candidate linked to the LTβR-TRAF3 pathway (Supplemental Fig. 1E). EWS is an RNA binding protein that participates in miRNA production (20, 21), splicing, and mRNA transport [Reviewed in (22)]. Indeed the EWS:TRAF3 complex has been detected by others using a yeast-two-hybrid screen (23), which gave us confidence in our AP-MS results. However, the novel link between EWS and the LTβR-TRAF3 pathway required validation.

EWS disassociates from TRAF3 upon stimulation and is required for optimal responsiveness to LTβR activation

We first proceeded to validate the TRAF3:EWS complex with biochemical methods. Indeed using tagged proteins, we detected the association of EWS (endogenous and MYC-tagged) with FLAG-TRAF3 (Fig. 2A). In contrast, as predicted by the inverse relationship between EWS and TRAF2 in our BN (Fig. 1B), we could not detect the association of EWS with FLAG-TRAF2. These results verified our AP-MS data, while demonstrating the specificity of the EWS:TRAF3 complex.

Next we proceeded to verify the association of TRAF3 with EWS using endogenous proteins isolated from HeLa cells, in the presence or absence of LTβR signaling. For stimulation, we used recombinant LIGHT in place of agonistic anti-LTβR antibody to prevent interference with immunoprecipitation. Using this design, we detected peak association of TRAF3 with EWS (Fig. 2B) in unstimulated cells. Following LIGHT stimulation, we measured a significant decrease in the association of TRAF3 with EWS (Fig. 2C). One potential caveat to our experimental design is that LIGHT can also ligate Herpesvirus Entry Mediator (HVEM), which is the TNFRSF member with the highest shared sequence homology with LTβR. However, LIGHT stimulation of HeLa cells signal through LTβR due to the lack of HVEM expression on the cell surface (24). Taken together, these results validate the association of EWS with TRAF3 using endogenous protein and demonstrate that this complex is influenced by LTβR signaling.

We evaluated the impact of EWS depletion on LTβR signaling, using an NF-κB luciferase reporter system in HEK293T (Fig. 2D). In this system, receptor clustering is induced via over-expression, which is a common method used for studying TNFRSF member signaling *in vitro* (25). In control cells transfected with an empty vector and shRNA targeting EWS (shEWS) we measured increased NF-κB activity (p-value = 2.17×10^{-2}), versus cells expressing a control shRNA (shCtrl). This suggested that EWS might have a suppressive role in unstimulated cells, which is either directly or indirectly linked to the NF-κB pathway. In contrast, we measured a 28% decrease of NF-κB activation by LTβR in cells expressing shEWS, versus cells expressing shCtrl (p-value = 5.99×10^{-3}), suggesting that EWS is

required for peak NF-κB activation by LTβR. Interestingly, NF-κB activity induced by over-expression of HVEM did not differ between shCtrl and shEWS conditions. Although the differential impact of shEWS on LTβR and HVEM mediated activation of NF-κB may not be directly comparable due to differences in peak activation. It is possible that these observations may be due to signaling differences. For example, while both HVEM and LTβR can recruit TRAF2 and activate classical NF-κB activity, TRAF3 and the alternative NF-κB pathway do not respond to HVEM signaling (26). Moreover, depletion of EWS also reduces NF-κB activity downstream of Nucleotide-binding oligomerization domain-containing protein 2 signaling (27), which also activates the alternative NF-κB pathway (28). Taken together, the differences with HVEM and similarities with Nucleotide-binding oligomerization domain-containing protein 2 signaling suggested that EWS influences activation of the alternative NF-κB pathway.

To determine if EWS has a role in the alternative NF-κB pathway, we stimulated control and EWS-depleted NHDF with agonistic anti-LTβR antibody and measured p52 accumulation by western blot (Fig. 2E). We compared the stimulation-dependent responsiveness of p52 levels for each knockdown condition and included p100 levels as variable for normalization by multivariate linear regression (adjusted $R^2 = 0.973$; p-value = 2.96×10^{-11}). In control cells (Fig. 2F), we measured increased p52 accumulation at two hours post LTβR stimulation (p-value = 7.21×10^{-3}), which continued through to six hours (p-value = 1.28×10^{-4}). In EWS-depleted cells (Fig. 2F), no significant change in p52 was detected (p-value = 1.4×10^{-1}) at two hours post stimulation. However, at six hours increased p52 was detected (p-value = 7.61×10^{-6}), suggesting that activation is reduced at early time points, but recovers by six hours. Interestingly, in EWS-depleted cells, a trend towards increased p52 levels appeared in unstimulated cells (p-value = 2.2×10^{-1}), which resembled the elevated basal NF-κB activity in HEK293T expressing shEWS (Fig. 2D). These observations, along with the apparent defects in early p100 processing, suggested that EWS maintains normal LTβR signaling, perhaps by suppressing signaling in unstimulated cells.

EWS limits GM-CSF and ERK-2 levels for LTβR pathway

Although NF-κB is a critical part of the LTβR pathway, we expanded our study to explore other potential functions for EWS. Using a multiplex gene expression inflammation panel by NanoString, we assayed for differential expression of genes between control and EWS-depleted NHDF, stimulated with anti-LTβR antibody for zero, two, and six hours. Of the 255 genes assayed, 99 genes showed significant (adjusted p-value < 1.0×10^{-1}) differences due to knockdown or stimulation conditions (Supplemental Fig. 2A). NF-κB signaling genes, TRAF2, RIPK2, and BIRC2 were significantly increased in EWS-depleted cells, while TNFAIP3 and NFKB1 were reduced. However, these genes represented a minor fraction of the total number of genes measured and may not capture the main effect of EWS depletion on signaling.

To identify representative genes, we used hierarchal clustering on PCA (Fig. 3A), which identified a group of genes (Fig. 3B) enriched in cells depleted of EWS (v test = 2.17 for shEWS). Pathway enrichment analysis predicted that these genes have functions in regulating “Signaling of Interleukins”, “MAPK targets/Nuclear events mediated by MAP

kinases", and "PID P38 ALPHA BETA DOWNSTREAM PATHWAY" (Supplemental Fig. 2B). EWS depletion elevated the expression of ERK-2 (also known as MAPK1), a key signaling enzyme, which prompted us to measure active phospho-ERK-2 (Fig. 3C). Knockdown of EWS (Fig. 3D) significantly increased phospho-ERK-2 (p-value = 4.56×10^{-3}), which was also induced by LTβR stimulation at 15 minutes (p-value = 1.23×10^{-8}) and 30 minutes (p-value = 5.18×10^{-7}). This observation is in agreement with the increased *ERK-2* detected by NanoString in EWS-depleted NHDF. In contrast, we did not detect any significant impact to phospho-ERK-1 levels (Fig. 3E) due to knockdown of EWS (p-value = 9.9×10^{-1}), despite significant induction at 15 minutes (p-value = 7.42×10^{-6}) and 30 minutes (p-value = 2.46×10^{-5}) post LTβR stimulation. Taken together, our observations suggested that EWS is required to maintain normal levels of ERK-2 signaling protein.

Since LTβR signaling is critical for shaping the local extracellular environment in lymphoid tissue, we were curious if loss of EWS also results in a change to secreted proteins. Indeed, the NanoString data shows that depletion of EWS increased expression of *GM-CSF* in response to LTβR stimulation (Fig. 3B). To verify this observation, as shown in Figure 3F, we measured the expression of *GM-CSF* in NHDF by quantitative RT-PCR. In control knockdown cells, *GM-CSF* was weakly induced at two hours post stimulation (p-value = 1.47×10^{-5}) and remained unchanged at six hours. In unstimulated cells, depletion of EWS significantly increased *GM-CSF* (p-value = 1.15×10^{-4}), which was unchanged at two hours post stimulation. At six hours post stimulation, an additional increase to *GM-CSF* was measured in EWS-depleted NHDF (p-value = 2.61×10^{-3}). These results validate the increased *GM-CSF* mRNA levels detected in our NanoString data.

To determine if depletion of EWS also impacted the production of GM-CSF protein, we measured levels in supernatants using the Luminex platform (Fig. 3G), which has minimum detectable dose of 0.155 pg/ml. In the supernatants of unstimulated control NHDF, we measured 4.4 pg/ml of GM-CSF, which is similar to levels detected in bronchoalveolar lavage fluid isolated from idiopathic lung disease patients (29) or in the sera of burn patients (30). Following LTβR stimulation for 24 hours, levels increased an additional 0.8 pg/ml (p-value = 3.0×10^{-2}). In the supernatants of unstimulated cells depleted of EWS using two different shRNAs, we measured 4.9 (shEWS A; p-value = 2.34×10^{-6}) and 8.9 (shEWS B; p-value = 1.22×10^{-7}) pg/ml of GM-CSF. Following LTβR stimulation for 24 hours, these cells secreted an additional 1.2 (shEWS A; p-value = 3.0×10^{-2}) and 2.6 (shEWS B; p-value = 1.0×10^{-3}) pg/ml of GM-CSF, representing a 1.5- to 3.25-fold increase in GM-CSF, when compared to control cells. These results demonstrated that EWS maintains normal LTβR function by limiting production of GM-CSF.

We posit a role for EWS in the LTβR-TRAF3 pathway that begins with formation of the TRAF3:EWS complex in unstimulated cells. Following LTβR ligation, EWS released from TRAF3, can then translocate to the nucleus to repress the transcription of *ERK-2* and *GM-CSF*. Alternatively, many of the mRNAs elevated in EWS-depleted cells, including *ERK-2 (MAPK1)*, have been reported to associate with EWS (31). This suggests a role for the RNA binding activity of EWS (Supplemental Figs. 2C–D), which may help to remove mRNAs through direct destabilization or indirectly via its miRNA scaffolding function (20).

Others have shown that prolonged activation of ERK signaling reduces stimulation-dependent activation of NF-κB (32, 33), suggesting that minimal ERK-2 in basal conditions is critical for optimal responsiveness to LTβR signaling. Although our studies show that defects in NF-κB activation appear to resolve by six hours post stimulation. This may not be the case in secondary lymphoid organs, where LTβR signaling is constitutively active. A study with *Ews*-null mice revealed disproportionately small thymi, spleens and a cell-autonomous defect in pre–B cell development (34); however, further characterization is required to ascribe these defects to changes in NF-κB or ERK activation. Moreover, understanding the physiological consequences of LTβR signaling in *Ews*-null mice may provide insight into how this pathway contributes to immune function.

Supplementary Material

Refer to Web version on PubMed Central for supplementary material.

Acknowledgements

We thank Drs. Wai Lin and Caroline Stienne for helpful discussions.

This research was supported in part by NIH grants (CA164679, AI067890, CA177322) awarded to CFW. RVS is a recipient of an NIH Rheumatic Diseases Training grant (T32AR064194). Additional funds provided by the Jean Perkins Foundation and a research contract with Boehringer Ingelheim, Inc.

Abbreviations used in this article

LTβR	Lymphotoxin β receptor
AP-MS	Affinity-Purification Mass Spectrometry
EWS	Ewing's sarcoma
NHDF	Normal Human Dermal Fibroblasts
WGCNA	Weighted correlation network analysis
BN	Bayesian Network
HEK293T	Human embryonic kidney 293T
TRAF2	TNF receptor-associated factor 2
TRAF3	TNF receptor-associated factor 3
LIGHT	Tumor necrosis factor ligand superfamily member 14
p100	NF-κB-2
HVEM	Herpesvirus Entry Mediator
NIK	NF-κB-inducing kinase

References

1. Sedy J, Bekiaris V, and Ware CF 2014 Tumor necrosis factor superfamily in innate immunity and inflammation. Cold Spring Harb Perspect Biol 7: a016279. [PubMed: 25524549]
2. Shih VF, Tsui R, Caldwell A, and Hoffmann A 2011 A single NFkappaB system for both canonical and non-canonical signaling. Cell Res 21: 86–102. [PubMed: 21102550]
3. Sanjo H, Zajonc DM, Braden R, Norris PS, and Ware CF 2010 Allosteric regulation of the ubiquitin:NIK and ubiquitin:TRAF3 E3 ligases by the lymphotoxin-beta receptor. J Biol Chem 285: 17148–17155. [PubMed: 20348096]
4. Browning JL 2008 Inhibition of the lymphotoxin pathway as a therapy for autoimmune disease. Immunol Rev 223: 202–220. [PubMed: 18613838]
5. Ishida S, Yamane S, Ochi T, Nakano S, Mori T, Juji T, Fukui N, Itoh T, and Suzuki R 2008 LIGHT induces cell proliferation and inflammatory responses of rheumatoid arthritis synovial fibroblasts via lymphotoxin beta receptor. J Rheumatol 35: 960–968. [PubMed: 18412315]
6. Braun A, Takemura S, Vallejo AN, Goronzy JJ, and Weyand CM 2004 Lymphotoxin beta-mediated stimulation of synoviocytes in rheumatoid arthritis. Arthritis Rheum 50: 2140–2150. [PubMed: 15248211]
7. da Silva Antunes R, Madge L, Soroosh P, Tocker J, and Croft M 2015 The TNF Family Molecules LIGHT and Lymphotoxin alphabeta Induce a Distinct Steroid-Resistant Inflammatory Phenotype in Human Lung Epithelial Cells. J Immunol 195: 2429–2441. [PubMed: 26209626]
8. Bienkowska J, Allaire N, Thai A, Goyal J, Plavina T, Nirula A, Weaver M, Newman C, Petri M, Beckman E, and Browning JL 2014 Lymphotoxin-LIGHT pathway regulates the interferon signature in rheumatoid arthritis. PLoS One 9: e112545. [PubMed: 25405351]
9. VanArsdale TL, VanArsdale SL, Force WR, Walter BN, Mosialos G, Kieff E, Reed JC, and Ware CF 1997 Lymphotoxin-beta receptor signaling complex: role of tumor necrosis factor receptor-associated factor 3 recruitment in cell death and activation of nuclear factor kappaB. Proc Natl Acad Sci U S A 94: 2460–2465. [PubMed: 9122217]
10. Teo G, Liu G, Zhang J, Nesvizhskii AI, Gingras AC, and Choi H 2014 SAINTexpress: improvements and additional features in Significance Analysis of INTeractome software. J Proteomics 100: 37–43. [PubMed: 24513533]
11. Mellacheruvu D, Wright Z, Couzens AL, Lambert JP, St-Denis NA, Li T, Miteva YV, Hauri S, Sardiu ME, Low TY, Halim VA, Bagshaw RD, Hubner NC, Al-Hakim A, Bouchard A, Faubert D, Fermin D, Dunham WH, Goudreault M, Lin ZY, Badillo BG, Pawson T, Durocher D, Coulombe B, Aebersold R, Superti-Furga G, Colinge J, Heck AJ, Choi H, Gstaiger M, Mohammed S, Cristea IM, Bennett KL, Washburn MP, Raught B, Ewing RM, Gingras AC, and Nesvizhskii AI 2013 The CRAPome: a contaminant repository for affinity purification-mass spectrometry data. Nat Methods 10: 730–736. [PubMed: 23921808]
12. Scutari M 2009 Learning Bayesian networks with the bnlearn R package. arXiv preprint arXiv:0908.3817.
13. Højsgaard S 2012 Graphical independence networks with the gRain package for R. Journal of Statistical Software 46: 1–26. [PubMed: 22837731]
14. Pahlich S, Zakaryan RP, and Gehring H 2008 Identification of proteins interacting with protein arginine methyltransferase 8: the Ewing sarcoma (EWS) protein binds independent of its methylation state. Proteins 72: 1125–1137. [PubMed: 18320585]
15. Sanz H, Aponte JJ, Harezlak J, Dong Y, Ayestaran A, Nhabomba A, Mpina M, Maurin OR, Diez-Padrisa N, Aguilar R, Moncunill G, Selidji Todagbe A, Daubenberger C, Dobano C, and Valim C 2017 drLumi: An open-source package to manage data, calibrate, and conduct quality control of multiplex bead-based immunoassays data analysis. PLoS One 12: e0187901. [PubMed: 29136653]
16. Love MI, Huber W, and Anders S 2014 Moderated estimation of fold change and dispersion for RNA-seq data with DESeq2. Genome Biol 15: 550. [PubMed: 25516281]
17. Langfelder P, and Horvath S 2008 WGCNA: an R package for weighted correlation network analysis. BMC Bioinformatics 9: 559. [PubMed: 19114008]
18. Falcon S, and Gentleman R 2006 Using GOstats to test gene lists for GO term association. Bioinformatics 23: 257–258. [PubMed: 17098774]

19. Bista P, Zeng W, Ryan S, Bailly V, Browning JL, and Lukashev ME 2010 TRAF3 controls activation of the canonical and alternative NFkappaB by the lymphotoxin beta receptor. J Biol Chem 285: 12971–12978. [PubMed: 20185819]
20. Ouyang H, Zhang K, Fox-Walsh K, Yang Y, Zhang C, Huang J, Li H, Zhou Y, and Fu XD 2017 The RNA binding protein EWS is broadly involved in the regulation of pri-miRNA processing in mammalian cells. Nucleic Acids Res 45: 12481–12495. [PubMed: 30053258]
21. Kim KY, Hwang YJ, Jung MK, Choe J, Kim Y, Kim S, Lee CJ, Ahn H, Lee J, Kowall NW, Kim YK, Kim JI, Lee SB, and Ryu H 2014 A multifunctional protein EWS regulates the expression of Drosha and microRNAs. Cell Death Differ 21: 136–145. [PubMed: 24185621]
22. Kovar H 2011 Dr. Jekyll and Mr. Hyde: The Two Faces of the FUS/EWS/TAF15 Protein Family. Sarcoma 2011: 837474. [PubMed: 21197473]
23. Wang J, Huo K, Ma L, Tang L, Li D, Huang X, Yuan Y, Li C, Wang W, Guan W, Chen H, Jin C, Wei J, Zhang W, Yang Y, Liu Q, Zhou Y, Zhang C, Wu Z, Xu W, Zhang Y, Liu T, Yu D, Zhang Y, Chen L, Zhu D, Zhong X, Kang L, Gan X, Yu X, Ma Q, Yan J, Zhou L, Liu Z, Zhu Y, Zhou T, He F, and Yang X 2011 Toward an understanding of the protein interaction network of the human liver. Mol Syst Biol 7: 536. [PubMed: 21988832]
24. Cheung TC, Coppieters K, Sanjo H, Oborne LM, Norris PS, Coddington A, Granger SW, Elewaut D, and Ware CF 2010 Polymorphic variants of LIGHT (TNF superfamily-14) alter receptor avidity and bioavailability. J Immunol 185: 1949–1958. [PubMed: 20592286]
25. Chang YH, Hsieh SL, Chen MC, and Lin WW 2002 Lymphotoxin beta receptor induces interleukin 8 gene expression via NF-kappaB and AP-1 activation. Exp Cell Res 278: 166–174. [PubMed: 12169272]
26. Cheung TC, Steinberg MW, Oborne LM, Macauley MG, Fukuyama S, Sanjo H, D'Souza C, Norris PS, Pfeffer K, Murphy KM, Kronenberg M, Spear PG, and Ware CF 2009 Unconventional ligand activation of herpesvirus entry mediator signals cell survival. Proc Natl Acad Sci U S A 106: 6244–6249. [PubMed: 19332782]
27. Warner N, Burberry A, Franchi L, Kim YG, McDonald C, Sartor MA, and Nunez G 2013 A genome-wide siRNA screen reveals positive and negative regulators of the NOD2 and NF-kappaB signaling pathways. Sci Signal 6: rs3. [PubMed: 23322906]
28. Pan Q, Kravchenko V, Katz A, Huang S, Ii M, Mathison JC, Kobayashi K, Flavell RA, Schreiber RD, Goeddel D, and Ulevitch RJ 2006 NF-kappa B-inducing kinase regulates selected gene expression in the Nod2 signaling pathway. Infect Immun 74: 2121–2127. [PubMed: 16552041]
29. Carraway MS, Ghio AJ, Carter JD, and Piantadosi CA 2000 Detection of granulocyte-macrophage colony-stimulating factor in patients with pulmonary alveolar proteinosis. Am J Respir Crit Care Med 161: 1294–1299. [PubMed: 10764326]
30. Hur J, Yang HT, Chun W, Kim JH, Shin SH, Kang HJ, and Kim HS 2015 Inflammatory cytokines and their prognostic ability in cases of major burn injury. Ann Lab Med 35: 105–110. [PubMed: 25553289]
31. Zhu Y, Xu G, Yang YT, Xu Z, Chen X, Shi B, Xie D, Lu ZJ, and Wang P 2019 POSTAR2: deciphering the post-transcriptional regulatory logics. Nucleic Acids Res 47: D203–D211. [PubMed: 30239819]
32. Maeng YS, Min JK, Kim JH, Yamagishi A, Mochizuki N, Kwon JY, Park YW, Kim YM, and Kwon YG 2006 ERK is an anti-inflammatory signal that suppresses expression of NF-kappaB-dependent inflammatory genes by inhibiting IKK activity in endothelial cells. Cell Signal 18: 994–1005. [PubMed: 16242916]
33. Carter AB, and Hunninghake GW 2000 A constitutive active MEK --> ERK pathway negatively regulates NF-kappa B-dependent gene expression by modulating TATA-binding protein phosphorylation. J Biol Chem 275: 27858–27864. [PubMed: 10878013]
34. Li H, Watford W, Li C, Parmelee A, Bryant MA, Deng C, O'Shea J, and Lee SB 2007 Ewing sarcoma gene EWS is essential for meiosis and B lymphocyte development. J Clin Invest 117: 1314–1323. [PubMed: 17415412]

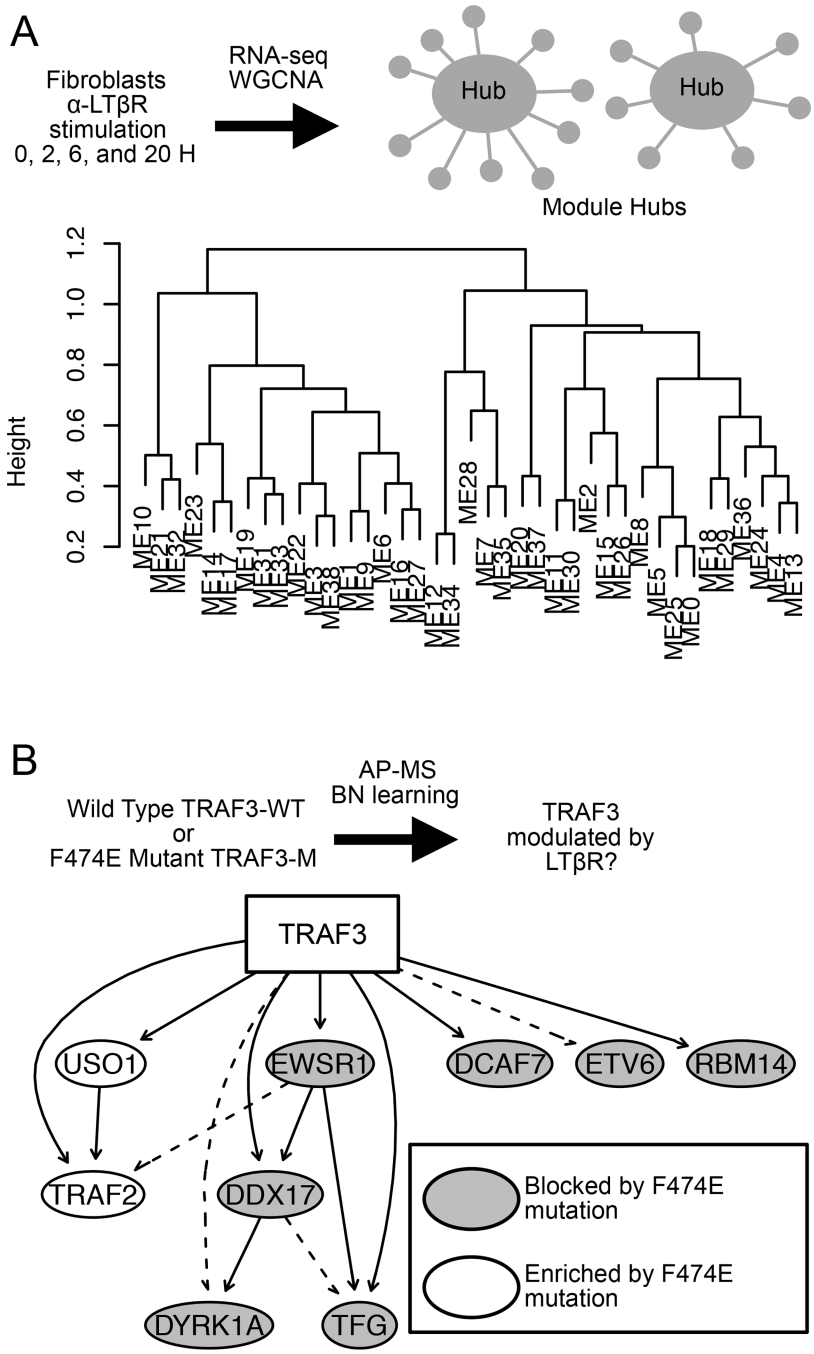

FIGURE 1.

'Omics screen links *EWSR1* to LTβR-TRAF3 pathway. (**A**) Top, the workflow used to detect hubs in NHDF undergoing active LTβR signaling. Bottom, a dendogram showing modules detected by WGCNA. (**B**) Top, the workflow used to detect TRAF3 complexes. Bottom, a BN summarizing the detected complexes. Dashed edges indicate protein complexes that are inversely related.

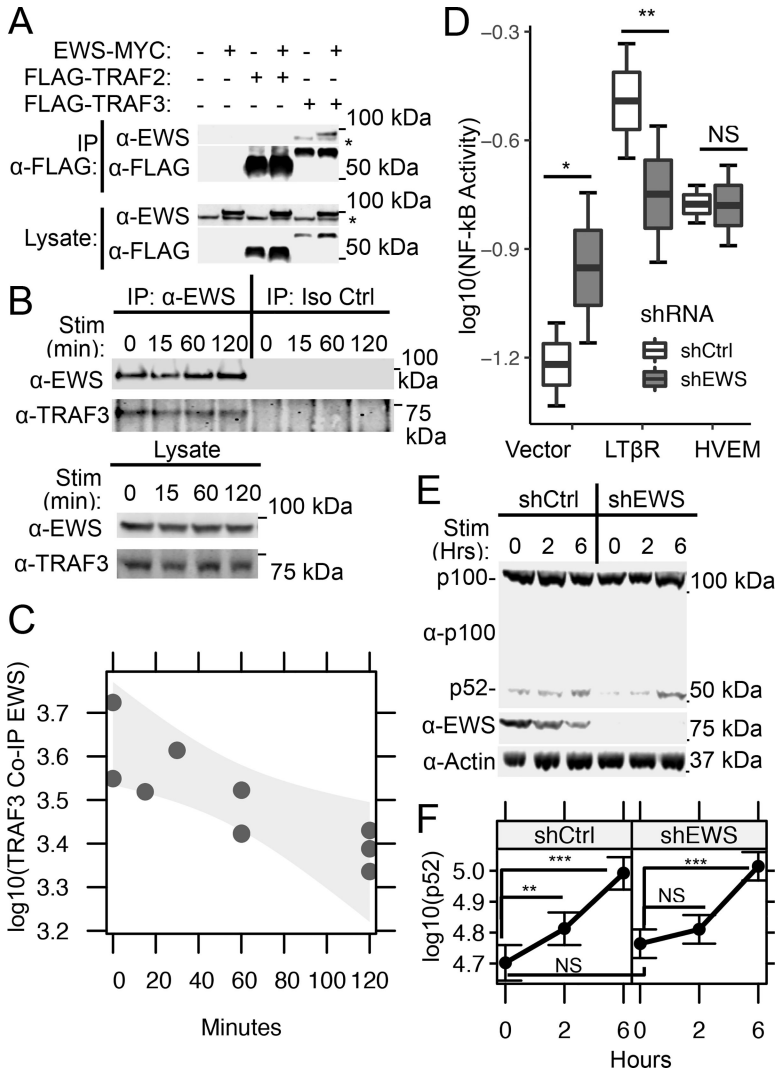

FIGURE 2.

EWS disassociates from TRAF3 upon stimulation and is required for optimal responsiveness to LTβR activation. (**A**) EWS-MYC associates with FLAG-TRAF3, but not FLAG-TRAF2 from HEK293T cells as shown by western blot. Endogenous EWS is indicated (*). Blot representative of three experiments. (**B**) TRAF3 associates with EWS isolated from HeLa cells at different times after LTβR stimulation (10 ng/ml recombinant LIGHT) as shown by western blot. (**C**) Regression shows the negative relationship between EWS-associated TRAF3 with Time. Levels quantified from three experiments. (**D**) A plot shows the impact of EWS depletion on NF-κB reporter activity in HEK293T cells transfected with empty vector or vectors expressing LTβR or HVEM. NF-κB activity measured as firefly luciferase activity, normalized to renilla luciferase control from two experiments. (**E**) Western blot shows the impact of EWS knockdown by shRNA on p52 accumulation in NHDF. Stimulation was carried out using 2 μg/ml agonistic anti-human LTβR antibody. (**F**) Regression shows the impact of EWS depletion on p52 accumulation quantified by western blot from two separate experiments. Error bars represent 95% confidence intervals.

Significance codes: *** < 0.001, ** < 0.01, * < 0.05, NS > 0.05. Positions of molecular weight makers are shown for cropped blots.

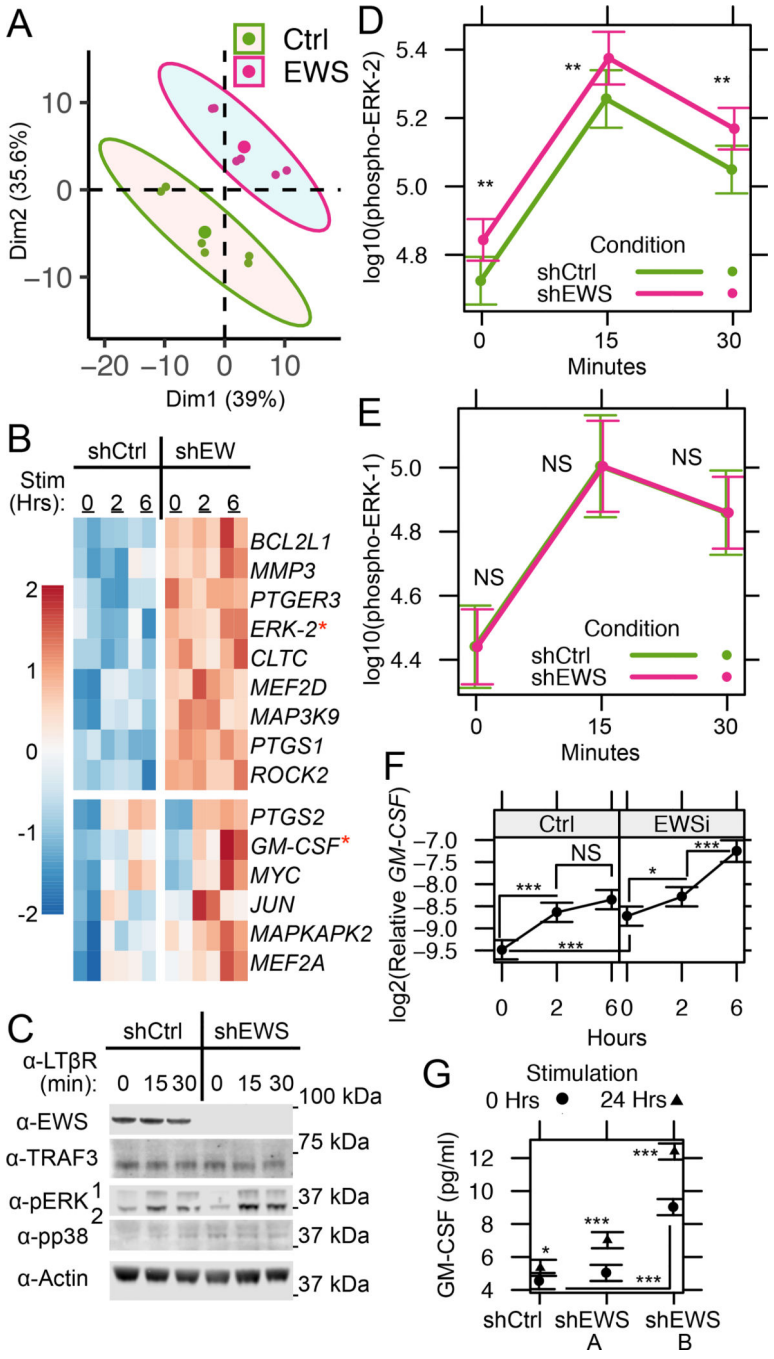

FIGURE 3.

EWS limits GM-CSF and ERK-2 levels for LTβR pathway in NHDF. (**A**) PCA plot showing the grouping of samples using the normalized expression levels for all differentially expressed genes. Ellipses represent 90% confidence. (**B**) A heatmap shows normalized NanoString data (scaled by row) for genes enriched during EWS knockdown conditions. (**C**) A representative western blot shows the impact of EWS knockdown on the induction of phospho-ERK-1 and phospho-ERK-2 following LTβR stimulation of NHDF. Regression shows the impact of EWS depletion on phospho-ERK-2 (**D**) and phospho-ERK-1 levels (**E**).

Levels quantified from three experiments. (**F**) Regression shows the impact of EWS depletion on *GM-CSF (L32* normalized*)* transcript following LTβR stimulation. Levels quantified from three experiments. (**G**) Regression shows the impact of EWS depletion on the secretion of GM-CSF follow LTβR stimulation. Levels quantified from two experiments. Error bars represent 95% confidence intervals. Significance codes: *** < 0.001, ** < 0.01, * < 0.05, NS > 0.05. Red asterisks on heatmap indicate genes of interest selected for validation. Western blot images were cropped. Positions of molecular weight makers are shown.